Adsorbate phonons on Ni(100)(1×1)-H

H. Okuyama, M. Z. Hossain, T. Aruga, and M. Nishijima*
Department of Chemistry, Graduate School of Science, Kyoto University, Kyoto 606-8502, Japan
(Received 13 June 2002; published 17 December 2002)

We have investigated vibrational states of H on Ni(100)(1×1)-H by means of electron energy loss spectroscopy (EELS). In addition to the symmetric stretch mode at 645 cm^{-1}, we detect an asymmetric stretch mode at ~700 cm^{-1} near the $\bar{\Gamma}$ point. This mode is found to be collective and exhibits a dispersion up to 850 cm^{-1} at the $\bar{X}$ point. It is characterized by an anomalously large linewidth (~150 cm^{-1}) whose origin is discussed on the basis of the experimental results.

DOI: 10.1103/PhysRevB.66.235411 PACS number(s): 68.35.Ja, 68.43.Pq

I. INTRODUCTION

Hydrogen on metal surfaces is a prototype of the adsorption system and attracts much attention because of the fundamental as well as technological interest. The vibrational property, in particular, has been a central issue because of its relevance to the dynamical processes such as diffusion and reaction, and has been investigated on a variety of surfaces.[1] A wealth of vibrational spectra have been accumulated to date by using electron energy loss spectroscopy (EELS).

For the threefold coordinated H adatoms on face-centered-cubic (fcc) (111) surfaces, the two fundamental modes have been readily observed in the vibrational spectra, corresponding to the symmetric (ν_s) and asymmetric (ν_{as}) stretch modes.[1,2] On the other hand, there exist only two studies to our knowledge which could determine the ν_{as} for the fourfold coordinated H adatoms on fcc(100) probably due to the sensitivity problem; the primary energy should be carefully optimized to detect the asymmetric modes of the fourfold coordinated H [Pd(100) (Ref. 3) and Rh(100) (Ref. 4].

The adsorbed state of H on Ni(100) has been studied by means of low-energy electron diffraction (LEED), EELS,[5,6] and He diffraction.[7] In the earlier LEED study at 200 K,[5] a quasiordered $p(2\times2)$ pattern was observed at medium coverages. In the following LEED study at 100 K,[6] similar streaky features with significant background intensity were observed, but no well-defined extra spot was observed. With increasing exposure, the background intensity decreases and a (1×1) pattern with a sharp contrast [as for the clean Ni(100)] was observed, which was confirmed by the He diffraction experiments.[7] The vibrational states were investigated by EELS, and a single dipole-active loss was observed at 78 meV (630 cm^{-1}) at the saturation coverage which was assigned as the symmetric stretch mode of H adatoms adsorbed in the fourfold hollow sites of Ni(100).[5,6] Thus, it was suggested that H adatoms are disorderedly arranged at low coverages and a well-defined (1×1)-H structure is formed at the saturation. The adsorption states were also studied by the first-principles density-functional calculations,[8,9] which were in reasonable agreement with the experimental results.

In this study, we investigate the vibrational states of H on Ni(100) mainly at the saturation coverage. In addition to the symmetric stretch mode previously observed,[5,6] we detect an asymmetric stretch mode at ~700 cm^{-1} near the $\bar{\Gamma}$ point, which disperses up to 850 cm^{-1} at the $\bar{X}$ point. It is found that the linewidth of the asymmetric mode is markedly large (~150 cm^{-1}) in contrast to that of the symmetric mode (~30 cm^{-1}), the origin of which is discussed in terms of quantum delocalization, vibrational damping and surface inhomogeneity.

II. EXPERIMENTAL

The experiments were carried out using an ultrahigh vacuum chamber equipped with a high-resolution electron energy loss spectrometer (LK-5000, LK Technologies, Inc.), a four-grid retarding-field analyzer for LEED, and a quadrupole mass spectrometer for thermal desorption measurements. A Ni(100) sample was cleaned by cycles of 500 eV Ar ion sputtering and 1100 K annealing. For the clean surface, a sharp (1×1) LEED pattern was obtained. We prepared the H(D)-covered sample by exposing the clean surface at 90 K to $H_2(D_2)$ via a tube doser. The exposure is given by the background $H_2(D_2)$ pressure multiplied by time in units of L (1 L=1×10^{-6} Torr s). The surface is saturated with H adatoms at 10 L of $H_2(D_2)$, where the (1×1)-H(D) structure is formed. All measurements were conducted at the sample temperature of 90 K. The primary electron energy E_p, incidence angle θ_i, and emission angle θ_e (with respect to the surface normal) were varied depending on the experiments. The electrons were scattered along the [011] direction of Ni(100). The energy resolution of 16–24 cm^{-1} (2–3 meV) was used.

III. RESULTS

Figure 1 shows a series of EELS spectra for Ni(100)(1×1)-H measured along the $\bar{\Gamma}\bar{X}$ direction of the surface Brillouin zone. The spectra are shown as a function of the parallel momentum transfer $Q_\parallel$ which is varied by rotating the analyzer towards the off-specular direction. The momentum transfer is represented by $\zeta \equiv Q_\parallel / K_{\bar{X}}$, where $K_{\bar{X}}$ = 1.261 $Å^{-1}$. The E_p is 20 eV, and θ_i is 80° for the upper two spectra and 70° for the others. Two dispersing features are observed below 300 cm^{-1} which are ascribed to Ni phonons.[10] At higher energy, we observe losses which are ascribed to H vibrations. In the specular direction ($\zeta=0$), a

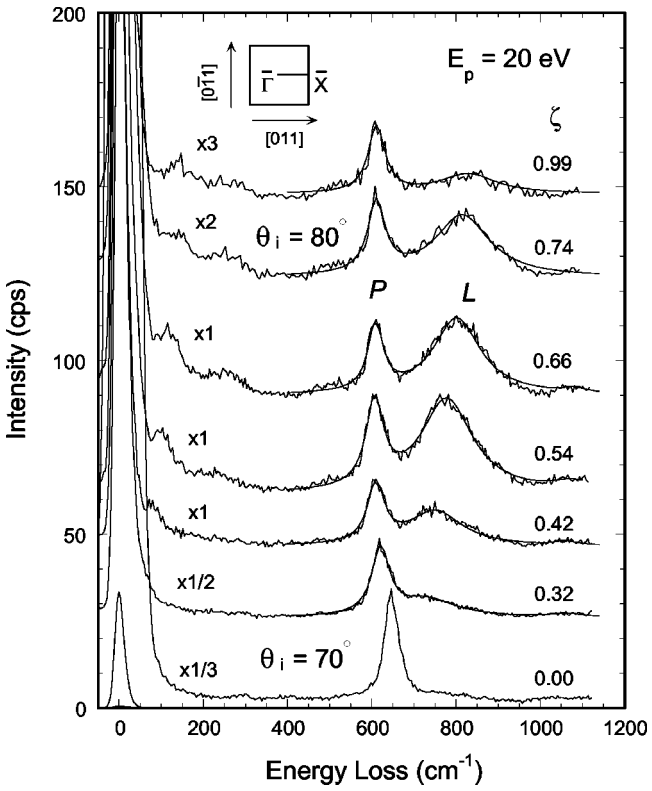

FIG. 1. A series of EELS spectra of Ni(100)(1×1)-H as a function of the normalized momentum transfer ζ along the $\overline{\Gamma X}$ direction of the surface Brillouin zone (shown in the inset). $\zeta=1$ corresponds to the $\overline{X}$ point. The primary energy E_p is 20 eV, and $\theta_i=80°$ for the upper two spectra and $\theta_i=70°$ for the others. The elastic peak is shown for $\zeta=0$ (intensity: 10^5 cps). The two main features are due to H vibrations, which are fitted with Lorentzian functions and represented by solid curves.

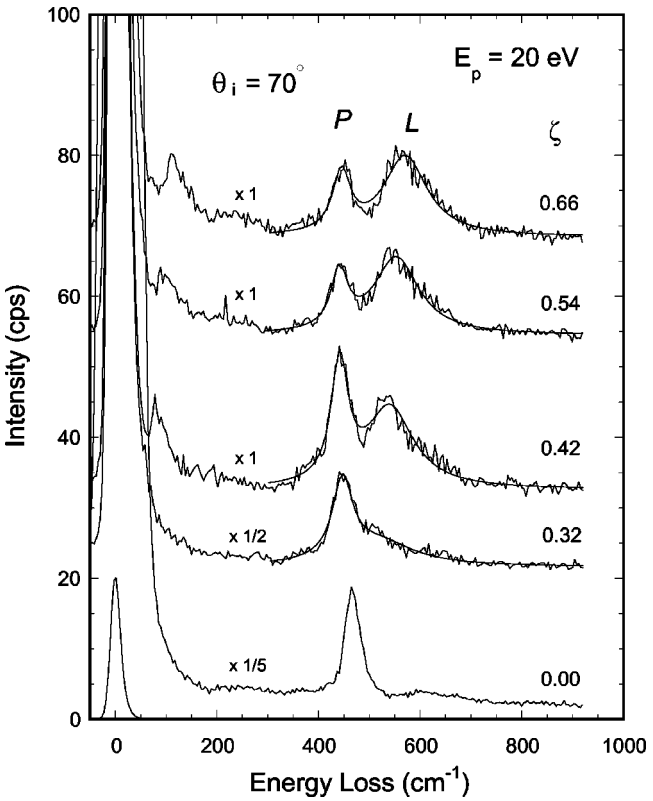

FIG. 2. A series of EELS spectra of Ni(100)(1×1)-D as a function of the normalized momentum transfer ζ along the $\overline{\Gamma X}$ direction of the surface Brillouin zone. The E_p is 20 eV and $\theta_i=70°$, and the elastic peak is shown for $\zeta=0$ (intensity: 10^5 cps). The two main features are due to D vibrations, which are fitted with Lorentzian functions and represented by solid curves.

single loss is observed at 645 cm^{-1}. The loss was observed at 630 cm^{-1} in the earlier studies,[5,6] which was assigned as the symmetric stretch mode of H (ν_s) adsorbed at the four-fold hollow site. The peak intensity decreases in the off-specular direction, which indicates that the mode is excited with the dipole mechanism;[11] the 645 cm^{-1} mode is confirmed to be the ν_s. It disperses downwards with increasing the momentum transfer, and thus, it is a collective excitation of the H adatoms (phonon) and assigned as a predominantly perpendicular-polarized transverse mode (denoted by P).

In the off-specular direction, we detect a distinct loss at higher energy which is first observed in this study. We can straightforwardly assign the loss as an asymmetric stretch mode of H (ν_{as}) because it is detected only in the off-specular direction.[11] It shows strong upward dispersion with increasing the momentum transfer. While the ν_{as} is doubly degenerate at the $\overline{\Gamma}$ point, the H-H interactions lift the degeneracy along the $\overline{\Gamma X}$ direction, generating two branches, i.e., the longitudinal and transverse modes predominantly polarized along the [011] and [0$\bar{1}$1] directions, respectively. The upward dispersion indicates that this is the longitudinal mode (denoted by L), while the transverse mode is not observed according to the selection rule of impact scattering of EELS.[11] In addition to these fundamental losses, a small feature is observed at ~1100 cm^{-1} which is ascribed to the overtone of ν_s (the two-phonon excitation of P). These H-derived peaks are fitted with three curves of Lorentzian functions as shown in the figure to determine the energies and intrinsic widths of the two fundamental modes. Figure 2 shows a series of EELS spectra for Ni(100)(1×1)-D. Isotope shifts (~1.4) are obvious both for P and L, confirming H/D motions involved in these modes. Because we cannot detect the overtone in this case, the spectra are fitted with two curves of Lorentzian functions as shown in the figure.

Figure 3 shows a series of EELS spectra for Ni(100)(1×1)-H at $E_p=25$ eV and $\theta_i=75°$, including the energy region of overtones. At this E_p, the intensity of the ν_s (P) is increased while that of the ν_{as} (L) is not so much changed. Correspondingly, the overtone of ν_s (the two-phonon excitation of P) is clearly observed at 1100 cm^{-1}. The mechanism of the enhancement is not investigated in this study, but it is probably associated with the resonance scattering of incidence electrons.[3,4] The corresponding spectra for D on Ni(100) are shown in Fig. 4, where the overtone is observed at 815 cm^{-1} around the zone edge. The loss at ~600 cm^{-1} observed in the spectra of $\zeta=0.12$–0.30 is ascribed to H adsorbed from the background.

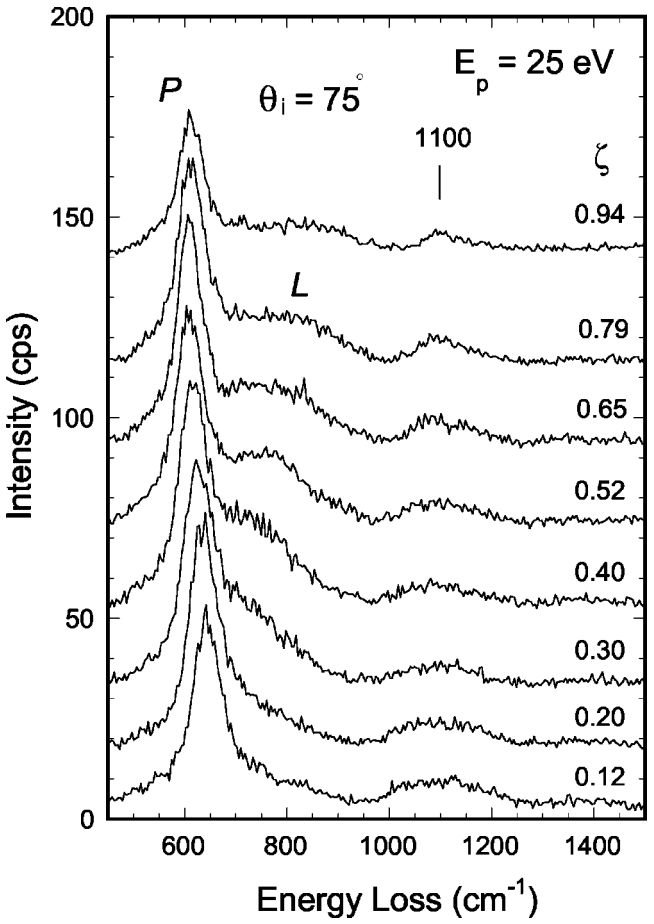

FIG. 3. A series of EELS spectra of Ni(100)(1×1)-H at $E_p = 25$ eV and $\theta_i = 75°$. The perpendicular-polarized mode at ~ 600 cm^{-1} is intensified at this E_p, enabling the detection of the corresponding overtone at 1100 cm^{-1}.

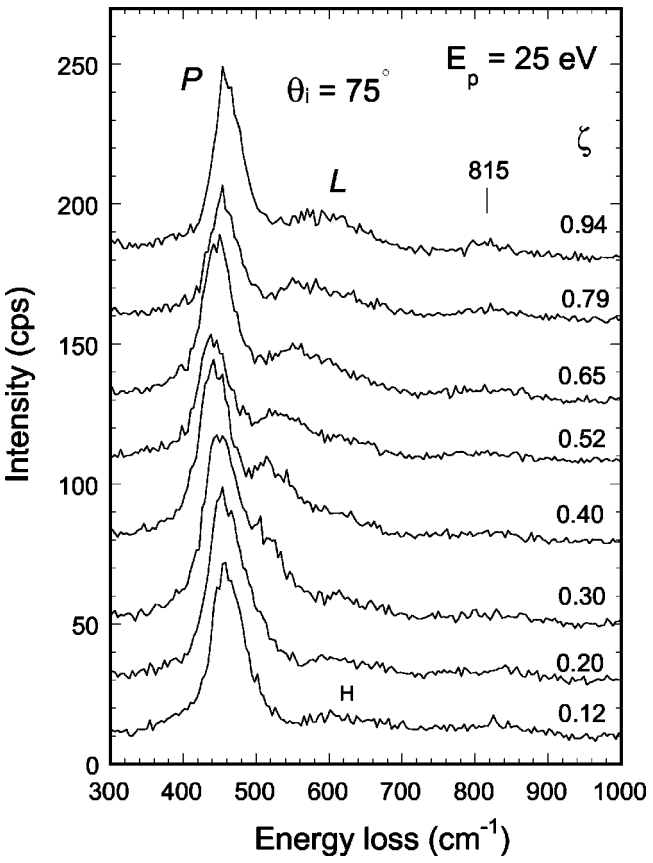

FIG. 4. A series of EELS spectra of Ni(100)(1×1)-D at $E_p = 25$ eV and $\theta_i = 75°$. The perpendicular-polarized mode at ~ 450 cm^{-1} is intensified at this E_p, enabling the detection of the corresponding overtone at 815 cm^{-1} near the zone boundary.

The loss energies and deduced intrinsic widths are shown in Fig. 5 as a function of ζ. If we consider one-dimensional array of oscillators interacting between the first- and second-nearest neighbors, the dispersions are simply fitted to cosine curves with three parameters: $\epsilon_0 + \epsilon_1 \cos(\pi\zeta) + \epsilon_2 \cos(2\pi\zeta)$. The results of the fittings are shown with the solid curves in Fig. 5(a). The parameter ϵ_0 corresponds to the vibrational energy of a decoupled oscillator, and ϵ_1 and ϵ_2 are related to the interactions between the first- and second-nearest neighbors in the array, respectively. The deduced parameters for H(D) are $\epsilon_0 = 619(451)$ cm^{-1}, $\epsilon_1 = 17(2)$ cm^{-1}, and $\epsilon_2 = 8(9)$ cm^{-1} for P, and $\epsilon_0 = 762(523)$ cm^{-1}, $\epsilon_1 = -87$ (-62) cm^{-1}, and $\epsilon_2 = 0(-10)$ cm^{-1} for L.

The intrinsic widths are determined from the full-widths at half-maxima (FWHM) of the fitted Lorentzian curves after deconvolution with the elastic peaks whose widths are between 16 and 24 cm^{-1}. The results are shown in Fig. 5(b). It is noted that the linewidths of L are ~ 150 and 100 cm^{-1} for H and D, respectively, which are anomalously large as compared to those of P (~ 30 cm^{-1}). The line-broadening mechanism will be discussed later.

We take the EELS spectra at lower coverages to investigate the vibrational states of more isolated H adatom species. Figure 6 shows the coverage dependence of the EELS spectra taken at $E_p = 9.5$ eV and $\theta_i = \theta_e = 70°$. The widths of the elastic peaks are ~ 18 cm^{-1}. The spectra are similar to those previously reported,[6] and thus, we briefly describe the coverage-dependent adsorbed states. Under this scattering condition, only the dipole-active mode (ν_s) is observed. At the initial stage of adsorption (0.02 L), two peaks appear which were ascribed to the isolated species (the lower-energy mode at ~ 550 cm^{-1}) and the (1×1)-H island species (the higher-energy mode at ~ 640 cm^{-1}) on the surface. The two adsorbed states always coexist at medium coverages, which indicates the existence of attractive interactions between H adatoms to form the (1×1)-H structure, as predicted by the recent density-functional study.[9] The isolated species dominates at 0.4 L. At the saturation (10 L), the surface is fully covered with the (1×1)-H structure and a single peak is observed at 645 cm^{-1} as described above. A small peak is observed at ~ 400 cm^{-1} which has been ascribed to slight trace of carbon.[6] The inset shows the spectra for 0.4 L exposure taken at $E_p = 20$ eV. The spectra (a) and (b) were taken with $\theta_i = \theta_e = 70°$, and $\theta_i = 70°$ and $\theta_e = 40°$, respectively. In the off-specular direction [spectrum (b)], a loss is observed at ~ 800 cm^{-1} which is assigned as the ν_{as} of the isolated H adatom species.

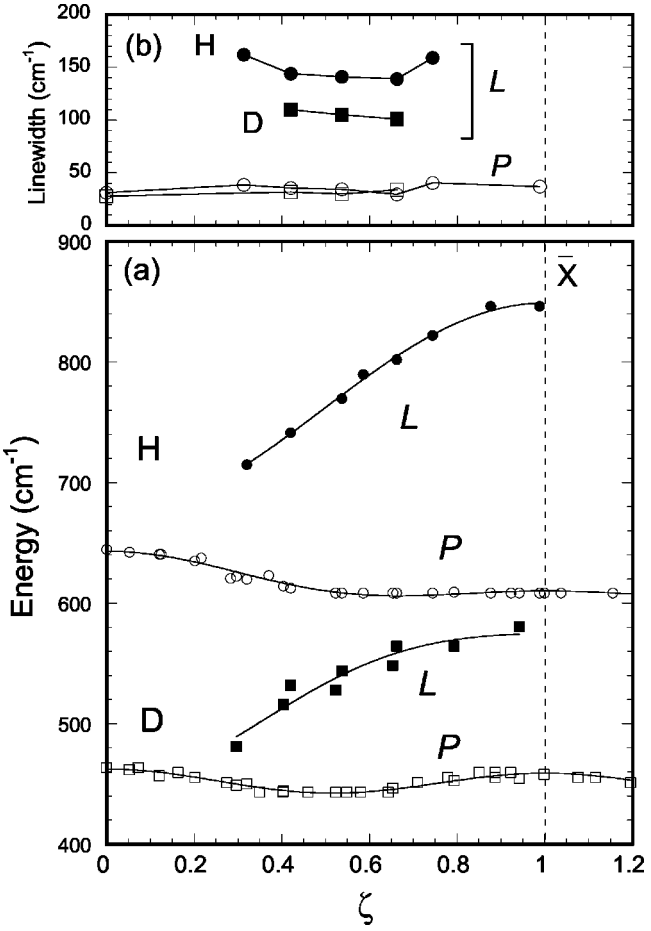

FIG. 5. (a) Dispersions of the vibrational energies of $\nu_s(P)$ and $\nu_{as}(L)$ for Ni(100)(1×1)-H(D) as a function of ζ. The solid curves are the results of fitting with cosine functions. Note that the local minimum at $\zeta \sim 0.5$ of ν_s (P) for D reflects the significance of the interactions between the second-nearest neighbors. (b) The intrinsic widths of the corresponding loss peaks are shown as a function of ζ.

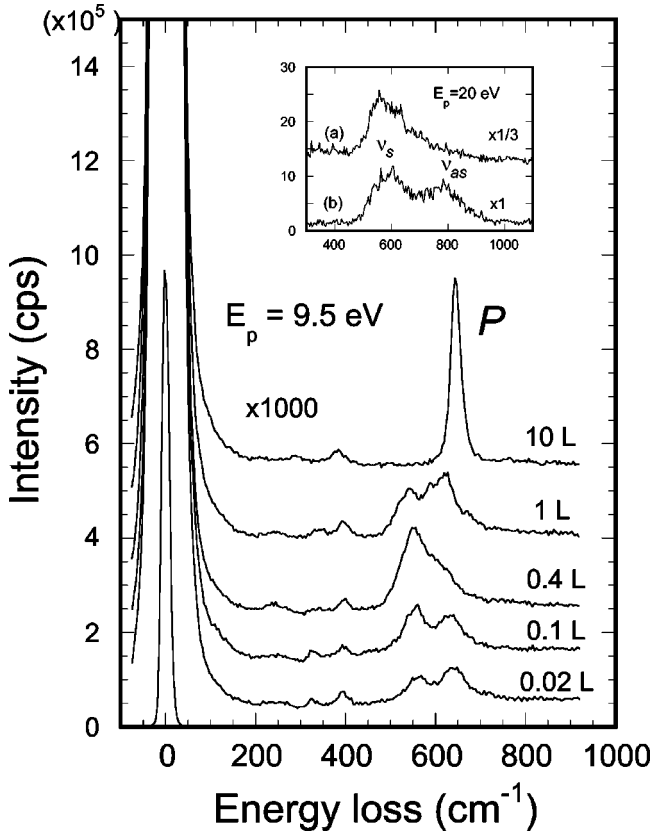

FIG. 6. Coverage-dependent EELS spectra for H on Ni(100) at $E_p = 9.5$ eV and $\theta_i = \theta_e = 70°$. The inset shows the spectra for 0.4 L exposure at $E_p = 20$ eV. The spectra (a) and (b) are taken with $\theta_i = \theta_e = 70°$, and $\theta_i = 70°$ and $\theta_e = 40°$, respectively.

IV. DISCUSSION

A. Fundamental vibrations and lateral interactions

The vibrational energies of H have been investigated on a variety of metal surfaces. We have determined the $\bar{\Gamma}$-point energies of L and P (ν_{as} and ν_s) of Ni(100)(1×1)-H to be ~700 and 645 cm^{-1}, respectively. Our results show that the ν_{as} is higher in energy than the ν_s for H on Ni(100). For H on Pd(100), the ν_{as} and ν_s were observed at 76 meV (610 cm^{-1}) and 63 meV (510 cm^{-1}), respectively,[3,12] and thus, this system also shows $\nu_{as} > \nu_s$. On the other hand, this relation is not applicable to H on Rh(100), where the ν_{as} and ν_s were observed at 65 meV (525 cm^{-1}) and 82 meV (660 cm^{-1}), respectively.[4] Thus the vibrational energies of the fourfold coordinated H are closely dependent on the chemical details of the H-surface interactions. This is in contrast to the case of three-fold coordinated H, which was proposed to show universally $\nu_{as} < \nu_s$.[2] The first-principles density-functional calculations predicted the ν_s and ν_{as} for the Ni(100)(1×1)-H at the $\bar{\Gamma}$ point to be 86 meV (695 cm^{-1}) and 68 meV (550 cm^{-1}), respectively,[8] which are deviated from the experimental results in particular for the ν_{as}.

The dynamical lateral interactions cause the dispersions of the fundamental modes at high coverage. The substantial contribution of ϵ_2 as well as ϵ_1 is obvious for P, which indicates a long-range nature of the interaction for this motion. This is consistent with the indirect mechanism of the interaction mediated by the substrate electrons which was predicted by the effective medium theory.[13] The downward dispersion of P can be qualitatively explained as follows: the upward displacement of H reduces the background charge density at the position of coadsorbed H, which causes the stiffening of the potential curve towards the vacuum.[13] Thus the in-phase motion along the surface normal ($\bar{\Gamma}$ point) is the highest in energy as shown in Fig. 5(a). Note that the local minimum at $\zeta \sim 0.5$ of P [Fig. 5(a)] reflects the significance of the interactions between the second-nearest neighbors. On the other hand, the short-range interaction dominates the L as deduced from $|\epsilon_1| \gg |\epsilon_2|$, and the upward dispersion indicates repulsion between the first-nearest neighbors in the out-of-phase motion.

B. Anharmonicity and two-phonon bound state

The observed energies of the overtone for Ni(100)(1×1)-H are shown in Fig. 7 as a function of ζ. The energies

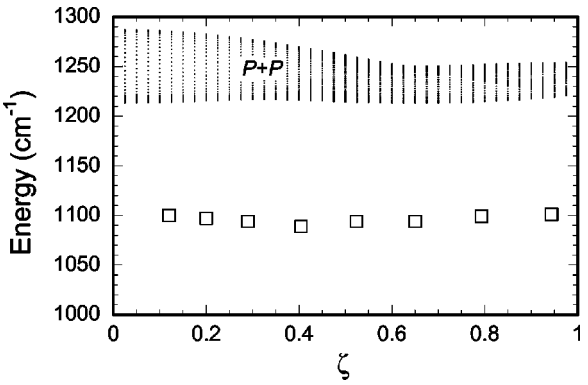

FIG. 7. Energies of the overtone of ν_s for Ni(100)(1×1)-H as a function of ζ. The overtone is interpreted to be a two-phonon bound state. Also shown is the corresponding free-two-phonon continuum $(P+P)$ calculated from the dispersion curve of P in Fig. 5(a).

are determined by fitting the peak shape to a curve of Lorentzian function. The free-two-phonon continuum generated from the double excitation of P is calculated, which is also shown in the figure $(P+P)$. It is obvious that the overtone is split off from the two-phonon continuum due to the anharmonicity, and thus, it is interpreted to be a two-phonon bound state with two quanta of vibrational excitations almost localized.[14] As shown in Fig. 3, the bound state is observed as a broad feature near the $\bar{\Gamma}$ point but is clearly seen as a sharp peak with increasing the momentum transfer. The origin of the broadening near the $\bar{\Gamma}$ point is not known yet. For D on Ni(100), the bound state is only seen near the zone boundary as shown in Fig. 4.

The two-phonon bound state exhibits little dispersion due to its localized character,[15] and the overtone energy of a decoupled H adatom ($\nu_s^{0\to 2}$) is estimated to be 1100 cm^{-1}. To determine the anharmonicity Γ (called $\hbar\omega_e\chi_e$ in general), the fundamental vibrational energy of a decoupled H adatom at the saturation coverage ($\nu_s^{0\to 1}$) should be known. The $\nu_s^{0\to 1}$ was estimated in the previous study,[6] where the ν_s was investigated as a function of the isotope concentration ratio. In the limit of zero concentration of H, the $\nu_s^{0\to 1}$ was deduced from the extrapolation to be 580 cm^{-1}.[6] Thus we can determine the anharmonicity $\Gamma=(2\nu_s^{0\to 1}-\nu_s^{0\to 2})/2$ to be 30 cm^{-1}.[11]

C. Line-broadening mechanisms

It is obvious that the L is characterized by an anomalously large linewidth ($\sim$150 cm^{-1}) in contrast to the relatively small width of P ($\sim$30 cm^{-1}). The line-broadening mechanisms of vibrations have been discussed mainly in terms of quantum delocalization,[16,17] lifetime broadening,[18–20] and inhomogeneous broadening.[21]

The delocalized vibrational states were theoretically predicted by Puska *et al.*[16] In their model, an H atom is considered to be a quantum particle due to its small mass, and thus, the vibrational excited states of H are delocalized along the surface and the vibrational spectra reflect its band-structured density of states (peak broadening). The weak corrugation of the potential is essential for the lateral tunneling and thus the delocalization of an H adatom. The model Hamiltonian for the excited states of H was proposed and represented as[22]

$$H=E\sum_i n_i^1+T\sum_{i,j} c_j^{\dagger 1}c_i^1+U\sum_i n_i^1 n_i^0+V\sum_{i,j} n_i^1 n_j^0, \tag{1}$$

where E corresponds to the vibrational energy of the isolated H adatoms, T is the hopping matrix element of the excited H adatoms between the nearest-neighbor sites, U is the repulsive energy when the excited H adatom shares a site with other H adatom in the ground state, and V is the repulsive energy between the excited adatom and the ground-state H adatom in the nearest-neighbor sites. The indices 1, 0, i, j denote the excited state, the ground state, a certain site in the system, and the nearest-neighbor sites of the site i, respectively. $c_i^{\dagger}(c_i)$ is the creation (annihilation) operator for the site i and $n_i=c_i^{\dagger}c_i$ is the occupation number of the site i. This Hamiltonian was solved for the systems of the one-dimensional array of H adatoms on Cu(110) (Ref. 22) and Pd(110).[23] For qualitative discussion, we neglect the contribution of V, and then, the Eq. (1) is represented as

$$H=\sum_i (E+Un_i^0)n_i^1+T\sum_{i,j} c_j^{\dagger 1}c_i^1. \tag{2}$$

We observe the transition of H from its ground state to the excited state at the site i', and thus, the Hamiltonian should be solved with $n_{i'}^0=0$. At first, we consider the case where n_i^0 is zero for the majority of i (low coverage). Then, the Hamiltonian yields delocalized states with the band-center energy E and localized states with the energy $(E+U)$. Obviously, the delocalization is hindered by the coadsorbed H adatoms, and thus, the broadening vanishes with increasing the coverage as supported experimentally.[22,23] On the other hand, in the case of saturation coverage where n_i^0 is one except for $n_{i'}^0$, the Hamiltonian yields delocalized states with the band-center energy $(E+U)$ and a localized state with the energy E at the site i'. At high coverage, the interactions between H adatoms cause a dispersion of the vibrational energy, which is superimposed on the broadening due to the delocalization.[17] In the present study of Ni(100)(1×1)-H, the observed linewidth of $\sim$150 cm^{-1} may be ascribed to the delocalization at the saturation coverage. We can consider the band-center energy $(E+U)$ to be equal to the energy of another H atom adsorbed on the Ni(100)(1×1)-H with respect to the ground-state H adatom in the Ni(100)(1×1)-H. The binding energy of the external H atom in the bridge (on-top) site on the saturated Pd(100)(1×1)-H surface was calculated to be -0.39 (-0.59) eV with respect to $\frac{1}{2}H_2$.[24] The binding energy for the fourfold coordinated H adatom in the Pd(100)(1×1)-H is calculated to be 0.47 eV with respect to $\frac{1}{2}H_2$,[24] and thus, the difference, i.e., $(E+U)$, is $\sim$1 eV ($\sim$8000 cm^{-1}). The observed energy of L ($\sim$700–850 cm^{-1}) is far below the expected value; the ν_{as} cannot be assigned to the delocalized state at $E+U$, but it is the localized state at E. Thus, another mechanism con-

tributes to the observed width of $\sim 150\ \mathrm{cm}^{-1}$. Note that the delocalized states with the band-center energy ~ 1 eV may exist and be observable with EELS, although the cross section of the transition is expected to be quite small.

While we suggest that the ν_{as} is localized in the (1×1)-H, it may be delocalized at lower coverage. With respect to this issue, we investigate the ν_{as} at low coverage and determine the energy to be $\sim 800\ \mathrm{cm}^{-1}$, as shown in the inset of Fig. 6. If the ν_{as} is delocalized at low coverage, we should observe a peak broadening with decreasing the coverage. It is observed that the ν_{as} shows a peak width comparable to that at high coverage [spectrum (b)]. Unfortunately, we cannot quantify the linewidth due to the complexity of the spectra caused by the coexistence of the two adsorbed states. The absence of measurable coverage-dependence of the peak shape may suggest that the ν_{as} is localized even at low coverage, i.e., $T \approx 0$ within our experimental error.

Although our study is focused on a well-defined overlayer of Ni(100)(1×1)-H, the inhomogeneous broadening may contribute to the observed width. The domain size of the (1×1)-H structure is finite on the real surface, which can cause the inhomogeneous broadening. Assuming the domain length of $\Delta x \sim 100$ Å, the uncertainty of the momentum $\Delta Q_{\parallel}$ is roughly estimated from $\Delta Q_{\parallel} \sim 1/\Delta x$ to be $\sim 0.01\ \text{Å}^{-1}$. From the dispersion curve in Fig. 5, $\Delta E < 3\ \mathrm{cm}^{-1}$ is deduced for L of H, indicating that the domain-size effect on the linewidth is negligible.

A minority species of H adatoms may exist around the defect sites, which can also cause the inhomogeneous broadening. Although the contribution from the surface defects is undoubtedly present, it is not compatible with the observed width as large as $\sim 150\ \mathrm{cm}^{-1}$. Furthermore, this mechanism cannot explain the mode-specific broadening. Thus, we suggest that the surface inhomogeneity contributes little to the width and another mechanism dominates the observed broadening.

We discuss a lifetime broadening via phonon damping process including another adsorbate mode, which has not received much attention except for a theoretical study[20] due to the experimental difficulty of detecting all the modes associated with the adsorbate. In this process, the higher-energy adsorbate mode (L) can decay via one substrate phonon and the other adsorbate mode (P) [denoted by Γ_2 (Ref. 20)] due to the anharmonic coupling. On the other hand, the lower-energy adsorbate mode can decay via an absorption of one substrate phonon and an emission of the other adsorbate phonon [denoted by Γ_3 (Ref. 20)]. Note that these processes are possible only in the case where the difference of the two adsorbate modes is within the maximum energy of the Ni substrate phonon ($295\ \mathrm{cm}^{-1}$).[25] The damping via an emission of two substrate phonons [denoted by Γ_1 (Ref. 20)] is not energetically allowed in the present case. It is obvious that the damping via Γ_2 is fast as compared to that via Γ_3 because the number of the substrate phonon is close to zero at 90 K. This leads to the dominant contribution of Γ_2 over Γ_3, and thus, only the higher-energy mode is effectively damped via this mechanism. In the theoretical prediction, the line broadening due to damping via Γ_2 is $\sim 20\ \mathrm{cm}^{-1}$ at 90 K for the case of O on Ni(100).[20] The anharmonic damping effect is larger for the vibrations with larger amplitudes (with smaller mass), and is proportional to the inverse of the reduced mass, $(m^{-1}+M^{-1})^{-1}$, where m and M are the masses of the adatoms and Ni, respectively.[19,26] Thus considering the predicted width of $\sim 20\ \mathrm{cm}^{-1}$ for O on Ni(100), the width of $\sim 150\ \mathrm{cm}^{-1}$ may be reasonable for H on Ni(100).

This interpretation of the linewidth is consistent with the case of H on Ni(111) (Ref. 14) and H on Ni(110).[27] For Ni(111)(1×1)-H, the L and P were observed at 920–1020 cm^{-1} and 1170–1140 cm^{-1} depending on the momentum transfer, and the higher-energy mode (P) exhibits an intrinsic width of $\sim 70\ \mathrm{cm}^{-1}$ in contrast to the L ($\sim 30\ \mathrm{cm}^{-1}$). For Ni(110)$(2\times1)$-H, the adsorbate modes were observed at ~ 640, ~ 870, and $\sim 1065\ \mathrm{cm}^{-1}$ with the width of 75, 100, and $150\ \mathrm{cm}^{-1}$, respectively.[17,27] The difference of the two adsorbate modes is within the maximum phonon energy of Ni for both cases, and the damping of the higher-energy mode via Γ_2 is possible.

V. CONCLUSION

We investigate the vibrational states for Ni(100)(1×1)-H by means of EELS. We detect an asymmetric stretch mode of H, which is interpreted to be a predominantly parallel-polarized longitudinal mode dispersing from ~ 700 to $850\ \mathrm{cm}^{-1}$ along the $\overline{\Gamma X}$ direction. The loss peak is characterized by an anomalously large width ($\sim 150\ \mathrm{cm}^{-1}$) in contrast to relatively small width observed for the perpendicular-polarized mode ($\sim 30\ \mathrm{cm}^{-1}$). Based on the experimental results, we discuss the origin of the broadening in terms of vibrational delocalization, vibrational damping and surface inhomogeneity. As a possible mechanism, we propose the vibrational-damping via two-phonon emission where the longitudinal mode decays with the excitation of a substrate phonon and the perpendicular-polarized mode of H.

ACKNOWLEDGMENTS

This work was supported in part by a Grant-in-Aid from the Ministry of Education, Science, Sports and Culture (Japan).

*Email address: nishijima@kuchem.kyoto-u.ac.jp

[1] K. Christmann, Surf. Sci. Rep. **9**, 1 (1988).
[2] L.J. Richter and W. Ho, Phys. Rev. B **36**, 9797 (1987).
[3] H. Conrad, M.E. Kordesch, W. Stenzel, M. Sunjić, and B. Trninic-Radja, Surf. Sci. **178**, 578 (1986).
[4] L.J. Richter, T.A. Germer, J.P. Sethna, and W. Ho, Phys. Rev. B **38**, 10 403 (1988).
[5] S. Andersson, Chem. Phys. Lett. **55**, 185 (1978).
[6] P.A. Karlsson, A.S. Mårtensson, S. Andersson, and P. Nordlander, Surf. Sci. **175**, L759 (1986).

[7] K.H. Rieder and H. Wilsch, Surf. Sci. **131**, 247 (1983).
[8] T.R. Mattsson, G. Wahnström, L. Bengtsson, and B. Hammer, Phys. Rev. **56**, 2258 (1987).
[9] G. Kresse and J. Hafner, Surf. Sci. **459**, 287 (2000).
[10] M. Rocca, S. Lehwald, H. Ibach, and T.S. Rahman, Surf. Sci. **171**, 632 (1986).
[11] H. Ibach and D.L. Mills, *Electron Energy Loss Spectroscopy and Surface Vibrations* (Academic Press, New York, 1982).
[12] H. Okuyama *et al.* (unpublished).
[13] P. Nordlander and S. Holmström, Surf. Sci. **159**, 443 (1985).
[14] H. Okuyama, T. Ueda, T. Aruga, and M. Nishijima, Phys. Rev. B **63**, 233404 (2001).
[15] J.C. Kimball, C.Y. Fong, and Y.R. Shen, Phys. Rev. B **23**, 4946 (1981).
[16] M.J. Puska, R.M. Nieminen, M. Manninen, B. Chakraborty, S. Holloway, and J.K. Nørskov, Phys. Rev. Lett. **51**, 1081 (1983); M.J. Puska and R.M. Nieminen, Surf. Sci. **157**, 413 (1985).
[17] W. Brenig, Surf. Sci. **291**, 207 (1993).
[18] J.W. Gadzuk and A.C. Luntz, Surf. Sci. **144**, 429 (1984).
[19] B.N.J. Persson, J. Phys. C **17**, 4741 (1984).
[20] J.C. Ariyasu, D.L. Mills, K.G. Lloyd, and J.C. Hemminger, Phys. Rev. B **30**, 507 (1984).
[21] R.G. Tobin, Surf. Sci. **183**, 226 (1987).
[22] C. Astaldi, A. Bianco, S. Modesti, and E. Tosatti, Phys. Rev. Lett. **68**, 90 (1992).
[23] N. Takagi, Y. Yasui, T. Takaoka, M. Sawada, H. Yanagita, T. Aruga, and M. Nishijima, Phys. Rev. B **53**, 13 767 (1996).
[24] S. Wilke, D. Hennig, R. Löber, M. Methfessel, and M. Scheffler, Surf. Sci. **307-309**, 76 (1994).
[25] R.J. Birgeneau, J. Cordes, G. Dolling, and A.D.B. Woods, Phys. Rev. **136**, A1359 (1964).
[26] D.C. Langreth and M. Persson, in *Laser Spectroscopy and Photochemistry on Metal Surfaces*, edited by H.-L. Dai and W. Ho (World Scientific, Singapore, 1995).
[27] B. Voigtländer, S. Lehwald, and H. Ibach, Surf. Sci. **208**, 113 (1989).